BIII-2

The Effect of Temperature and Strain-rate on the Deformation and Fracture of Mild-steel Charpy Specimens

T. R. Wilshaw[1] and P. L. Pratt[2]

ABSTRACT

The mechanics of the deformation in three-point bending of high-nitrogen mild-steel Charpy specimens was studied using the Fry's etch technique. Specimens were fractured with striker velocities of 0.05, 50 and 30,000 cm/min within a temperature range +100°C to -196°C. These studies revealed the existence of a) a transition from ductile tearing at the notch root to internal cleavage, b) at a lower temperature a bimodal energy behaviour in the region of slip-initiated cleavage and c) a decrease in fracture load associated with the onset of mechanical twinning.

The effect of strain-rate on these transitions may be expressed by Arrhenius equations with different activation energies, neither of which are equal to the activation energies for yielding at comparable stresses.

From these observations, and also from the results of instrumented Charpy tests performed on various mild steels, it is found convenient to identify a cleavage strength, σ_{CS}, which is the maximum longitudinal tensile stress below the notch root to cause cleavage. This cleavage strength must be dependent upon some micro-structural deformation features which do not influence the bulk plastic properties. It is proposed that σ_{CS} largely determines the value of the crack arrest temperature.

(1) Post-doctoral Research Assistant, Department of Metallurgy, Imperial College of Science and Technology, London, now at Department of Materials Science, Stanford University, Stanford, California.

(2) Professor of Crystal Physics, Department of Metallurgy, Imperial College of Science and Technology, London.

1. INTRODUCTION

The most common laboratory test for brittle fracture is the V-notch Charpy impact test. A rectangular prismatic bar containing a machined notch is broken in three-point bending with the notch in tension, under impact loading at various temperatures, and the energy absorbed during the fracture is measured. This energy changes considerably over a few tens of degrees as the fracture mode changes from ductile to cleavage. Brittle properties of materials are compared using various parameters obtained from this test based on either the fracture appearance or the amount of energy absorbed. However it is not known exactly what fundamental properties these parameters are estimating. From the aspect of design the use of Charpy data has met with some success, particularly in the design of ships, but each set of service conditions requires a new correlation with the test. Furthermore the inability to correlate data from different tests on a variety of steels, has made it desirable to analyse the Charpy test on a fundamental basis.

In this paper the state of stress around the notch is deduced from observations of the plastic zones, using Fry's reagent and application of slip-line field theory. Then by a systematic study of the effects of temperature and strain-rate on the deformation and fracture, some physical implications of the Charpy test are deduced and some of the characteristics of brittle cleavage are determined.

2. EXPERIMENTAL

Material

The material used throughout this work was a high-nitrogen mild steel of chemical composition:-

C	Mn	N	S	P
0.10/0.15	0.2	0.018	0.01	0.01

It was selected because of its property of reacting with Fry's reagent to reveal plastically deformed regions.

Standard Charpy specimens were machined strictly according to British Standard 131: Part 2 1959 from 1/2 inch square section rolled bar, and subsequently annealed at 850°C for 1 hour in an atmosphere of hydrogen and nitrogen.

The steel then had a uniform grain size of 40μ, with the cementite occurring in a massive coalesced form at the grain boundaries and also enveloping small islands of coarse pearlite.

Apparatus

The impact bend tests were performed on a 125 ft. lb. Avery impact machine, which had a striker velocity on impact of 16.5 ft/sec (30,000 cm/min), and which had been fitted with strain gauges by Fearnehough (1) to obtain load-time recordings. All other bend tests were carried out in a low temperature bending-jig attached to the cross-head of an Instron constant strain rate testing machine, Wilshaw (2).

The loads were recorded mechanically during the slow strain-rate tests, (striker velocity 0.05 cm/min) and on a cathode ray oscilloscope during the intermediate strain-rate tests (striker velocity 50 cm/min).

Uniaxial tensile properties were determined using Hounsfield test pieces pulled at normal strain-rates on the Instron, and at high strain-rates on an impact tensile machine constructed at the National Physical Laboratory by Harding (3).

3. THE LOAD-DEFLECTION CURVE

A typical room temperature load-deflection curve obtained by bending a Charpy specimen slowly is shown in Fig. 1. By continuous observation of a deforming specimen the small plastic instability or "yield-point" was seen to coincide with the sudden spread of arcs of plastic deformation (hereafter referred to as plastic "hinges") across the ligament. This state of strain represents the general yielding of the specimen and a continuous path of plastically deformed material can be traced across the section of the bar. The load at which this occurs is called the general yield load P_{GY} and it is proportional to the tensile lower yield stress of the material σ_{LYS}, Green and Hundy (4). Since this load represents a well defined position on the load-deflection curve, it is convenient to use it to define any point on the curve corresponding to a load P, by the ratio P/P_{GY}. For loads $P < P_{GY}$, this ratio, P/P_{GY}, is proportional to the ratio of the nominal stress at the notch root to the yield stress, σ/σ_Y, and it is in this form that we shall define points on the load-deflection curve.

Up to a load equivalent to $\sigma/\sigma_Y = 0.18$, the specimen deforms elastically throughout. At this load the nominal stress multiplied by the elastic stress concentration factor, $\alpha = 3.25$ after Neuber (5), becomes equivalent to the uniaxial yield stress of the material. As the load is increased further, the plastic zone spreads inwards from the notch root as revealed by Fry's etch in Fig. 1, and has the form of the logarithmic slip-line field predicted for pure four-point bending under plane strain, Wilshaw and Pratt (6). The longitudinal stress σ_X is distributed within the plastic zone according to Hill (7),

$$\sigma_X = 2k\left[1 + \ln(1 + x/r)\right] \qquad (1)$$

where x is the distance below the notch of root radius r, and k is the yield stress in shear, which for Tresca's criterion is $\sigma_Y/2$. The maximum longitudinal stress was related to the applied load through the experimentally determined plastic zone sizes and Equation 1, Wilshaw and Pratt (6). The maximum value of the plastic stress intensification factor, $\alpha = 1 + \ln(1 + x/r)$, is achieved before general yield at $\sigma/\sigma_Y = 0.8$; this experimental value is 2.05 ± 0.05 using the Tresca yield criterion. Between $\sigma/\sigma_Y = 0.8$ and general yield, the logarithmic slip field is surrounded by a region of "complementary" slip, and the value of the maximum stress remains constant even though the applied load is increasing (6).

At the upper general yield load, plastic "hinges" are nucleated, and their sudden propagation causes a small instability. Once general yielding has occurred the system becomes too complicated for a rigorous quantitative analysis. However the plastic strain patterns have been related to the bend angle in Fig. 1, and also to the value of the local plastic strain in the notch root, measured using a micro-hardness technique, Wilshaw (2). These measurements were used to estimate the local strain-rate in the root of the notch. At a striker velocity of 0.05 cm/min, the critial strain-rate was 3.8×10^{-3} sec^{-1} in the root, decreasing to a constant value of 1.8×10^{-3} sec^{-1} after 3° bend. Assuming that the strain-rate is proportional to the striker velocity, the strain-rate in the conventional impact test will be in the range 2300 sec^{-1} to 1000 sec^{-1}, which is consistent with previous estimates by Gensamer (8) and Hendrickson et al. (9). These strain-rate values are important since we shall be considering later the relationship between tensile and notch bend data.

4. THE FRACTURE LOAD-TEMPERATURE DIAGRAM

A schematic fracture load-temperature diagram, Fig. 2, was constructed from the results of load-deflection curves obtained over a wide range of temperatures and strain-rates, to represent all the deformation and fracture characteristics which were observed. The loads are presented as fractions of the general yield loads, so that it is possible to deduce the shape of the load-deflection curve, and the macroscopic strain pattern, at any temperature, from the previous analysis of the deformation characteristics.

The Ductility Transition, A-B

The abrupt decrease in the fracture instability load from A to B, Fig. 2, occurs at a well defined temperature T_d. Above T_d, the onset of instability is caused by the propagation of a ductile tear which originates at the root of the notch, Pratt and Wilshaw (10). Below T_d, microcracks are initiated by internal cleavage, causing instability before the plastic strain in the notch is sufficient for ductile tearing.

Prior to instability the stable microcracks become severely blunted by plastic deformation, and as a result they can be detected in the fracture profiles of the broken specimens. In this way cleavage was found to occur both above and below T_d. Hence the ductility transition is not simply due to a change in the mechanism of fracture initiation, but rather it represents a change in the mode of fracture, associated with the instability. Furthermore T_d is dependent on the size and geometry of the specimen, Stone and Turner (11), and therefore it cannot be a measure of any fundamental brittle property of the material.

Microscopical examination of both deformed and fractured specimens revealed that fractured cementite plates were directly responsible for the initiation of both cleavage (as observed by McMahon and Cohen (12)) and of ductile fractures. At the notch root the cementite fractures grow into small cavities which join together by internal necking to form a small tear, whilst the triaxial stress system below the notch root causes the cementite cracks to propagate, cleaving the ferrite matrix.

Little Fracture Beyond General Yield, B-C

As the temperature is decreased from T_d to that at which fracture and general yielding coincide, at C, instability occurs following successively smaller amounts of gross plastic deformation, the fracture load remaining approximately constant. In this region the stress required for cleavage is attained by strain-hardening. As the temperature decreases the yield stress of the material increases as shown by the dashed line for $\sigma/\sigma_Y = 1.0$, and cleavage will occur at smaller strains.

The Bimodal Transition Range, CD-EF

Between C and D, cleavage fracture occurs at the upper general yield load and the temperature dependence of the fracture load follows that of the general yield load. Within this same region fracture may occur significantly below the upper general yield load, at $\sigma/\sigma_Y \sim 0.8$, along EF.

At the slow and intermediate rates of strain this bimodal behaviour may be explained as a reflection of the state of stress below the notch root, assuming a critical tensile stress criterion of fracture, Wilshaw and Pratt (6). However at impact strain-rates the bimodality is more pronounced and cannot be explained on the same basis. The impact energy values measured directly from the machine vary with temperature according to Fig. 3. Between +20°C and +40°C the energy values fall into two definite groups separated by an energy gap of about 10 ft. lb. Crussard et al. (13) have observed a bimodal distribution which they attributed to a transition in the mode of fracture initiation from ductile tearing at the notch root to internal cleavage. This initiation transition occurs in the present work between 35 and 45 ft. lb., whereas both modes of fracture associated with the bimodality between 20°C and 40°C are initiated by cleavage.

The extent of plastic deformation in the broken specimens was revealed by Fry's reagent and representative patterns of the two modes of instability within the bimodal range are shown in Fig. 3. The low energy fractures always occurred prior to general yielding and the increase in energy from 5 to 15 ft. lb. within the bimodal range is due to an increase in post-brittle fracture energy. The high energy fractures all occurred well beyond general yield. The fracture and general yield loads are shown on the load-temperature diagram, Fig. 4. This diagram is different from any obtained by Fearnehough and Hoy (14) in so much as there is no region in which fracture occurred at the upper general yield load, in spite of the similarity in the yield stress temperature dependence.

The bimodality is not obvious from this diagram unless the specimen deflections are also considered. The work hardening rate is very small at these high strain-rates and consequently relatively large deflections accompany the fractures above general yield, so absorbing large amounts of energy. The difference in the energies to cause fracture instability was measured by integrating the load-time curve, and this is equivalent to the energy gap in the bimodal region.

This bimodal phenomenon does not seem to be associated with the stress distribution within the specimen because at low strain-rates fractures are observed at all states of strain above general yield. Alternatively this phenomenon may be a reflection of a fundamental transition in the mechanism of slip initiated cleavage. The concept of a transition from stable to unstable cleavage influenced by the role of grain boundaries seems attractive especially when the low strain-hardening capacity of the material at these high strain-rates is considered. However this concept is largely speculative and more detailed experiments on a variety of materials are necessary to establish the true nature of this bimodal phenomenon.

In this region CD-EF the temperature dependence of the maximum stress at fracture is equivalent to that of the lower yield stress. The bimodal transition temperature T_b is defined as the highest temperature at which fracture occurs before general yield. At T_b, the plastic stress intensification factor is at its maximum value, and this is a well defined position on the fracture load-temperature diagram. Above F, no mechanical twins were observed within the initiation zone, and hence fracture must be initiated by slip.

The Twinning Transition, E-F-G

Below F, there is a trend for the fracture load to decrease as the temperature decreases, together with a significant decrease in the value of σ/σ_y, Fig. 2. Similar behaviour has been reported by Knott and Cottrell (15) and Fearnehough and Hoy (14) who refer to this region FG as the fracture "cliff" or the low-stress fracture region.

A statistical survey of the distribution of twins in the impacted specimens whose fracture loads are presented in Fig. 4 was made in a more detailed way than that of Verbraak (16). At the estimated position of the maximum stress prior to instability, twins were observed in the region FG. The appearance of the twins together with the change in mechanical behaviour suggests that twinning is in some way responsible for the initiation of fracture in this region.

The decrease in stress intensification factor is precisely equivalent to the increase in the yield stress, and thus fracture appears to obey a constant critical tensile stress criterion in the region F-G.

5. THE EFFECT OF STRAIN-RATE ON THE FRACTURE LOAD-TEMPERATURE DIAGRAM

The fracture load-temperature diagrams obtained using striker velocities of 0.05 cm/min, 50 cm/min and 30,000 cm/min are presented in Figs. 4, 5, and 6 respectively. The overall effect of increasing the strain-rate is to cause the fracture load-temperature diagram to shift to higher temperatures. However, on more detailed inspection the actual form of the diagram is changed also. As the strain-rate increases the temperature dependence of the general yield load decreases and T_b approaches T_d, so that under impact straining part of BC and the whole of CD is missing from Fig. 2.

Arrhenius relationships between transition temperature and $\dot{\varepsilon}$ have been found by Wittman and Stepanov (17), Magnusson and Baldwin (18) and Vellinger and Wittwer (19) of the form

$$\dot{\varepsilon} = A \exp(-H/k\,T_t),$$

where H is the apparent activation energy,
k the Boltzmann constant,
and T_t the transition temperature.
The effect of strain-rate on various parameters at T_b and T_d is presented in Table 1. The values of T_b and T_d are plotted in the form ln $\dot{\varepsilon}$ vs $1000/T\ ^{o}K$ in Fig. 7. Both transitions obey an Arrhenius equation with the different apparent activation energies:-

$$H_{T_d} = 13{,}300 \pm 300 \text{ cal./mole}$$
$$= 0.58 \pm 0.02 \text{ eV},$$

and $$H_{T_b} = 5{,}100 \pm 200 \text{ cal./mole}$$
$$= 0.26 \pm 0.01 \text{ eV}.$$

The Strain-rate Sensitivity of T_b

The bimodal transition temperature is clearly defined on the fracture load-temperature diagram, and it represents the highest temperature at which slip-initiated cleavage occurs before the general yielding of the specimen. The sizes of the plastic zones around the notch root were measured in specimens fractured at T_b for the three strain-rates, and these were found to be equal. Thus according to Equation 1, the plastic stress intensification factor α_p is also equal, and on this basis it may be meaningful to compare fracture behaviour at T_b.

According to the ductile-brittle transition theories of Stroh (20), Cottrell (21), and Petch (22), the activation energy for the transition, based upon some dislocation model of cleavage initiation, should be equivalent to the activation energy for yielding. Arrhenius plots for three values of the lower tensile yield stress, 40, 50, and 60 Kg/mm^2, were made from experimental tensile data, and these are also shown in Fig. 7. The apparent activation energies for yielding at a constant stress

$$H_{LYS} = -k\left[\frac{d\,(\ln\dot{\varepsilon})}{d\,1/T}\right]_{\sigma_{LYS}}$$

were derived from the slopes of the three straight lines in Fig. 7. The values of σ_{LYS} measured by tensile tests at T_b for the predicted strain-rates at the notch, (Table 1), increase by 7 ± 4 Kg/mm^2 with a strain-rate increase of 10^6 sec^{-1}. Within the relevant stress range, 50-60 Kg/mm^2 (Table 1), there is a significant difference between H_{LYS} and H_{T_b}. Hence there appears to be no simple relationship between

discontinuous yielding and slip-initiated cleavage for this material. Dislocation theories assume that cleavage is initiated by a dislocation interaction mechanism whereas it has been established that ferrite cleavage is nucleated by cementite fracture in this steel. Consequently H_{Tb} may be more closely related to the activation energy for cleavage of cementite.

The Strain-rate Sensitivity of T_d

Lean and Plateau (23) measured H_{Td} from tensile tests and correlated their value with those obtained by other workers. They showed that H_{Td} is temperature dependent, obeying an equation, $H_{Td} = BT$ cals/mole, where B = 40-50 and T is the absolute temperature. Thus for T = 313 °K, H_{Td} = 12,500-15,500 cals/mole. This value agrees with that measured in the present work for Charpy specimens, but in our work H_{Td} was found to be independent of temperature. H_{Td} gives an empirical measurement of the strain-rate sensitivity of this transition, but there is evidence to suggest that it may be both size and temperature dependent. The value of H_{Td} is about twice H_{LYS}, Fig. 7, within the relevant range of yield stress values 40-60 Kg/mm^2, Table 1.

At T_d stable micro-cracks are found which are unable to propagate across the grain boundaries. The relaxation of the stress field at the tip of such a crack is related to the mobility of the dislocations which will be controlled to some degree by the strain-hardening characteristics of the material, Friedel (24). It is assumed that the cleavage stress σ_c is achieved by contributions from the yield stress σ_Y and a strain-hardening component $\Delta\sigma$, Cottrell (21), so that:- $\sigma_c \propto \sigma_Y + \Delta\sigma$. As the strain-rate increases $\Delta\sigma$ decreases and a greater contribution from the yield stress is required for cleavage.

The Maximum Longitudinal Stress Below the Notch

When cleavage occurs at T_d, i.e. above general yield, the maximum longitudinal stress below the notch may be calculated from $\sigma_{max} = \sigma_{LYS} \cdot \alpha_p$, where α_p is the stress intensification factor. Above general yield this will have a value of about 2.5 according to Knott (25). Then, applying the experimental values of σ_{LYS} obtained at T_d for the appropriate strain-rates (Table 1), increasing the strain-rate by 10^6 sec^{-1} has increased σ_{max} by about 50 Kg/mm^2 and T_d by 116°C,

i.e. $d\sigma_{max}/dT \approx + 0.4$ Kg/mm^2/°C
(the positive sign indicates increase with temperature)

However the resistance to cleavage increases with temperature, and therefore the value of $d\sigma_{max}/dT$ obtained in this way must be significantly influenced by the strain-rate. The high value of $d\sigma_{max}/dT$ obtained from yield stress measurements at T_d is caused by the unknown effect of strain rate and temperature on the strain-hardening behaviour associated with this transition.

From the results of Table 1, σ_{max} is proportional to the temperature T and to the logarithm of the strain-rate, ln $\dot{\varepsilon}$, so that

$$\sigma_{max} = \sigma_{max}\ (T,\ \ln \dot{\varepsilon}) \qquad (2)$$

At T_b, the micro-cracks are virile in the sense that they lead directly to fracture; thus it is reasonable to assume that strain-hardening will not affect cleavage at this temperature, i.e. $\Delta\sigma = 0$. Any effects of temperature and strain-rate on σ_{LYS} at T_b will be directly related to σ_{max} by the maximum stress intensification factor prior to general yield. According to Wilshaw and Pratt (6), $\alpha_p = 2.05 \pm 0.05$ at T_b. For this bimodal transition,

$$\frac{d\sigma_{max}}{dT} = \frac{d\sigma_{LYS}}{dTb} \cdot \alpha_p = +0.09 \pm 0.05 \text{ Kg/mm}^2/^\circ\text{C}$$

Differentiating Equation 2 with respect to T,

$$\frac{d\sigma_{max}}{dT} = \left(\frac{\delta\sigma_{max}}{\delta T}\right)_{\ln\dot{\varepsilon}} + \left(\frac{\delta\sigma_{max}}{\delta \ln\dot{\varepsilon}}\right)_T \cdot \frac{d \ln\dot{\varepsilon}}{dT} \qquad (3)$$

Because of the association between cementite cracks and ferrite cleavage, an estimate of the temperature dependence of the cleavage stress of the aggregate may be obtained from that for cementite fracture. Substituting the experimental value

$$\frac{d\sigma(\text{cementite})}{dT} = 0.15 \pm 0.05 \text{ Kg/mm}^2/^\circ\text{C}$$

into Equation 3, gives

$$\frac{d \ln\dot{\varepsilon}}{dT} \cdot \left(\frac{\delta\sigma_{max}}{\delta \ln\dot{\varepsilon}}\right)_T = +0.24 \pm 0.10 \text{ Kg/mm}^2/^\circ\text{C}$$

Using values from Table 1 for ln $\dot{\varepsilon}$ and T, a value of $\frac{d \ln\dot{\varepsilon}}{dT}$ can be estimated as

$$\frac{d \ln\dot{\varepsilon}}{dT} = \frac{2.303 \times 6}{165}\ ^\circ\text{C}^{-1}$$

Therefore $\left(\frac{\delta\sigma_{max}}{\delta \ln\dot{\varepsilon}}\right)_T = 2.8 \pm 1.1$ Kg/mm^2

measured within the range $3 \times 10^{-3} < \dot{\varepsilon} < 2 \times 10^3$ sec^{-1}.

In contrast to the observations of Hendrickson, Wood and Clark (26), the maximum longitudinal stress to cause cleavage is significantly strain-rate sensitive. This sensitivity makes it necessary to allow for strain-rate changes when attempting to predict impact transition temperatures from static tensile data.

6. DISCUSSION AND CONCLUSIONS

The main result of the analysis of the fracture behaviour in Section 5 is that the effects of temperature and strain-rate on the maximum longitudinal stress for cleavage are not simply due to their effects on the lower yield stress. We shall call this maximum longitudinal stress for cleavage the nominal cleavage strength of the material, σ_{cs}. It will be related to the true cleavage stress of the material by means of localised stress concentration factors of varying intensity caused by the inhomogeneity of the material e.g. dislocation configurations, mechanical twins, precipitates, etc.

Where slip dislocations alone are involved, the nominal cleavage strength should be related directly to the yield stress and the grain size of the material in the familiar manner. On the other hand, where other inhomogeneities of microstructure are present, in particular brittle precipitates either within the grains, or along the grain boundaries, the yielding behaviour of the matrix may be quite unimportant. Recently Allen et al. (27) have performed slow-bend tests on notched bars of alloy steels in various metallurgical conditions. Their inability to correlate the tensile proof stress with the nominal fracture stress in bending led to the suggestion that cleavage fracture in steels may be controlled by some property other than the conventional yield strength. They present experimental evidence which suggests that the nominal cleavage strength is size dependent. Therefore it is not a fundamental material property and cannot be used as a design criterion. However it may be a useful property to compare the toughness of different materials using test-pieces of the same size.

The pertinent questions still remain; what inherent material properties can be measured or estimated from the Charpy test and why do various materials have different transition temperatures? Instrumented Charpy tests have been performed by Fearnehough and Hoy (14), as well as in the present work, on a variety of mild steels which have 15 ft. lb. transition temperatures, T_{15}, ranging from $-90^{\circ}C$ to $+40^{\circ}C$. With only one exception the dynamic general yield load v. temperature curves were coincident, within the range of experimental scatter, for all these steels, in spite of their differing static yield stresses at room temperature. This phenomenon can be explained using the schematic diagram, Fig. 8. At low strain rates, $\sim 10^{-5}$, the yield stress is strongly temperature dependent in the region in which cleavage occurs. At the high strain-rates however, the yield stress has only a small temperature dependence, Fig. 8, and consequently any small variation in the nominal cleavage strength, σ_{cs}, will have a large resultant effect on the transition temperatures, T_A and T_B. This suggests that the nominal cleavage strength of the material may control the transition temperature, and conversely that the transition temperature is an indirect measure of the nominal cleavage strength. Therefore it would be valuable to discover what factors affect the cleavage strength.

If the propagation of a brittle crack consists of a series of separate initiations, Tipper (28), it seems likely that the cleavage strength will affect the crack propagation characteristics also. Further if the arresting of a crack can be considered as the inverse of crack initiation, then this too will be affected by the cleavage strength. The temperature at which a rapidly propagating brittle crack can be converted into a ductile crack is called the crack arrest temperature, T_{CAT}. This temperature is used as a safety design criterion and is determined experimentally by the Robertson test. This test involves the propagation of a brittle crack under a uniform stress, into a region of constant temperature, or into a region containing a temperature gradient; the temperature at which the crack changes from cleavage to ductile is estimated from the fracture appearance. Robertson tests were carried out on the high-nitrogen steel used in this work, and the gradient T_{CAT} was found to be $25 \pm 10^{\circ}C$.

It is interesting to look at the relationship between the crack arrest data and the Charpy data. The crack arrest temperature coincides with the bimodal energy region in Fig. 3, in which there is a sudden increase in the resistance to initiation by cleavage. This also coincides with the 15 ft. lb. transition temperature for the high-nitrogen steel, whereas Cowan and Vaughan (29) have shown that T_{CAT} is normally about $40^{\circ}C$ above the 15 ft. lb. transition temperature. Sharpening the machined notch by means of a fatigue crack in this high-nitrogen steel did not affect the bimodal transition temperature, T_b. This suggests that the effective strain-rate at the tip of a propagating brittle crack in the Robertson test is equivalent to that experienced by the material below the notch during the Charpy test, at least for this high nitrogen steel.

ACKNOWLEDGEMENTS

This work was financed by the Admiralty as part of a research programme on brittle fracture and supported by a Grant for Special Research from D.S.I.R. The authors would like to thank Professor J. G. Ball, the head of the Metallurgy Department of Imperial College for providing research facilities, Mr. G. D. Fearnehough of the U.K.A.E.A. for the use of an instrumented Charpy machine, and Dr. J. Harding and the N.P.L. for the use of an impact tensile machine. Mr. P. R. Christopher of the N.C.R.E. Rosyth helped throughout the work with advice and encouragement and also arranged the Robertson testing.

Many stimulating discussions were held with Dr. J. F. Knott, of the C.E.G.B., Dr. F. Guiu and the rest of our colleagues in the Metallurgy Department. Finally our thanks to Mr. K. Camichel for assistance with the experimental work.

REFERENCES

1. G. D. Fearnehough, U.K.A.E.A. Rep. 635 (c) 1963.
2. T. R. Wilshaw, Ph.D. Thesis, London University 1965.
3. J. Harding, J. Mech. Eng. Sc., 7, 2, 163, 1965.
4. A. P. Green and B. B. Hundy, J. Mech. and Phys. of Solids, 4, 128, 1956.
5. H. Neuber, "Theory of Notch Stresses", David Taylor Model Basin, U.S. Navy Translation 1946.
6. T. R. Wilshaw and P. L. Pratt, J. Mech. Phys. Sol., to be published.
7. R. Hill, Mathematical Theory of Plasticity, Clarendon Press, 1950.
8. M. Gensamer, Fracture of Metals, American Welding Soc. N.Y. 1947.
9. J. A. Hendrickson, D. S. Wood and D. S. Clark, Trans. A.S.M. 51, 629, 1959.
10. P. L. Pratt and T. R. Wilshaw, J.I.S.I., 202, 233, 1964.
11. D. E. W. Stone and C. E. Turner, Proc. Roy. Soc., A285, 83, 1965.
12. C. J. McMahon Jnr., and Morris Cohen, Acta Met., 13, 591, 1965.
13. C. Crussard, R. Borione, J. Plateau, Y. Morillon and F. Maratray, J.I.S.I., 183, 146, 1956.
14. G. D. Fearnehough and C. J. Hoy, ibid. 202, 912, 1964.
15. J. F. Knott and A. H. Cottrell, ibid. 201, 249, 1963.
16. C. A. Verbraak, Material-Prüfung, 3, 383, 1961.
17. F. Wittman and W. Stepanov, J. Tech. Phys. U.S.S.R., 9, 1070, 1939.
18. A. W. Magnusson and W. M. Baldwin Jnr., J. Mech. and Phys. of Solids, 5, 172, 1957.
19. K. Wellinger and J. Wittwer, Arch. Eisenhutt, 2, 125, 1963.
20. A. N. Stroh, Adv. in Physics, 6, 418, 1957.
21. A. H. Cottrell, Trans. A.I.M.E., 212, 192, 1958.
22. N. J. Petch, Phil. Mag., 3, 1089, 1958.
23. G. Lean and J. Plateau, Rév. de Met., 56, 427, 1959.

24. J. Friedel, "Fracture", Swampscott, Wiley, 498, 1959.
25. J. F. Knott, Ph.D. Thesis, Cambridge University 1962.
26. J. A. Hendrickson, D. S. Wood and D. S. Clark, Trans. A.S.M., 50, 656, 1958.
27. N. P. Allen, C. C. Earley and J. H. Rendall, Proc. Roy. Soc., A285, 120, 1965..
28. C. F. Tipper, J.I.S.I., 185, 4, 1957.
29. A. Cowan and H. G. Vaughan, Nucl. Eng., 7, 69, 1962.

Table 1

The effect of strain-rate on the ductility transition temperature T_d and the bimodal transition temperature T_b.

Striker velocity cm/min	0.05	50	30,000
Strain-rate in root predicted from micro-hardness measurements, sec^{-1}.	3×10^{-3}	3×10^{0}	2×10^{3}
The ductility transition temperature, T_d °C.	-76	-35	+40
$\frac{1000}{T_d}$ $^{o}K^{-1}$	5.07	4.20	3.18
Fracture loads at T_d P_F, kg.	1070 900	1200 1060	1300 1140
P_F/P_{GY} at T_d	1.410 1.20	1.43 1.26	1.37 1.20
General yield load at T_d P_{GY}, kg.	750	840	950
σ_{LYS} at T_d from tensile data at predicted $\dot{\varepsilon}$, kg/mm^2.	39 ± 1	48 ± 1	60 ± 3
Bimodal transition temperature T_b, °C.	-135	-86	+30
$\frac{1000}{T_b}$ $^{o}K^{-1}$	7.25	5.35	3.27
Decrease in σ/σ_y at T_b	1.0 0.66	1.0 ~0.7	~1.13 ~0.80
σ_{LYS} at T_b, kg/mm^2	53 ± 1	56 ± 1	60 ± 3

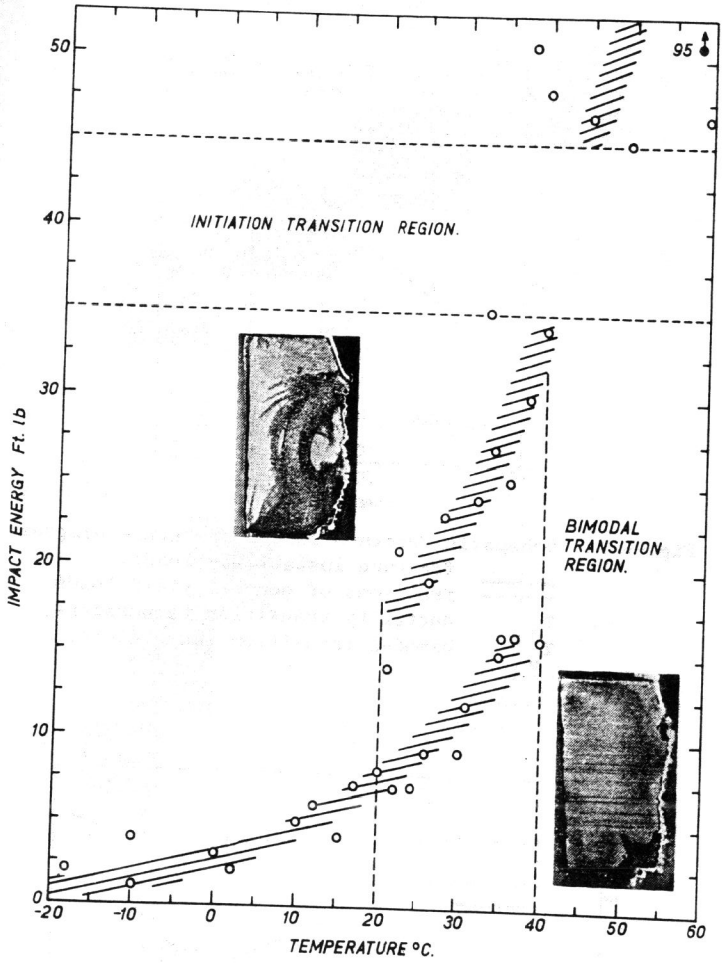

Figure 1. Schematic load-deflection diagram for a Charpy specimen under three-point bending at room temperature. The plastic strain patterns were revealed by Fry's reagent. (Notch depth = 2 mm.).

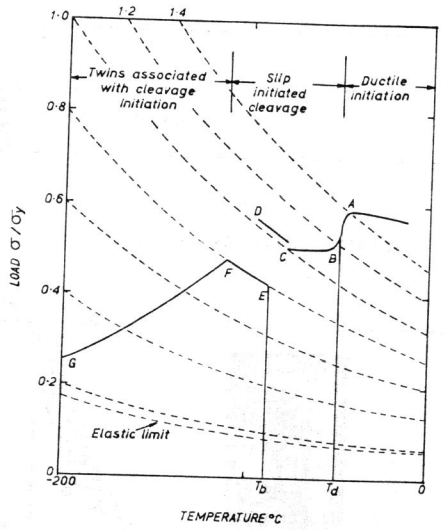

Figure 2. Schematic fracture load-temperature diagram.
——— fracture instability loads.
------ fractions of general yield loads.
T_d ductility transition temperature.
T_b bimodal transition temperature.

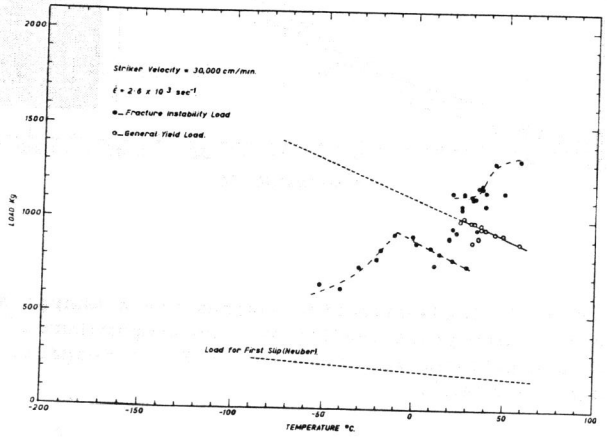

Figure 4. Fracture load-temperature diagram. Striker velocity 30,000 cm/min.

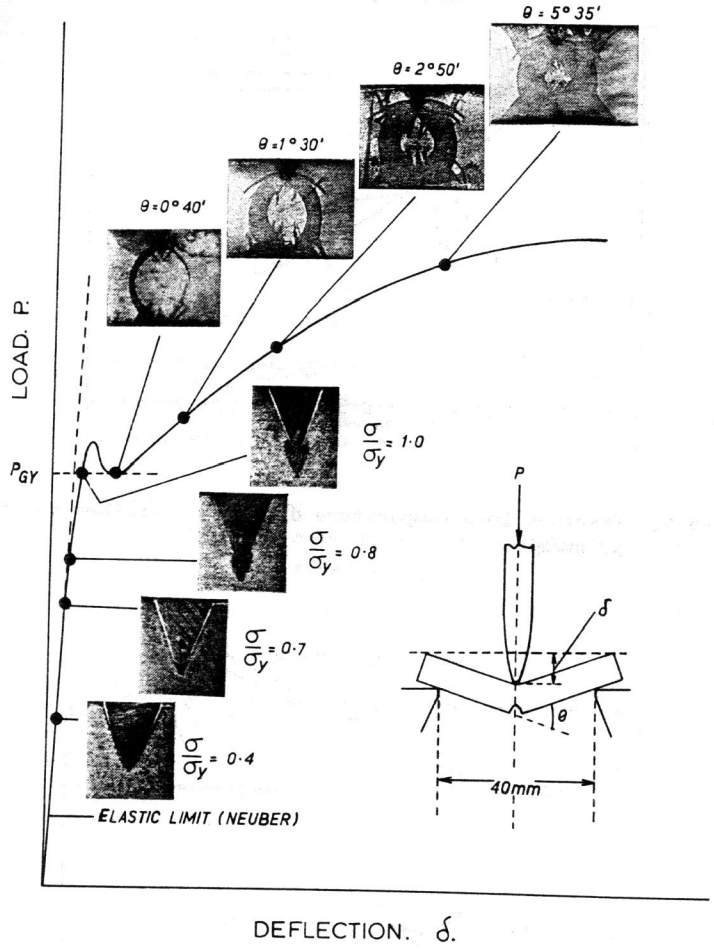

Figure 3. Charpy impact energy vs. temperature.

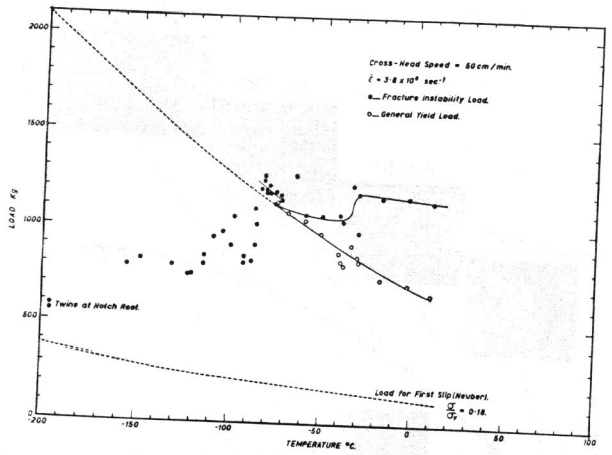

Figure 5. Fracture load-temperature diagram. Striker velocity 50 cm/min.

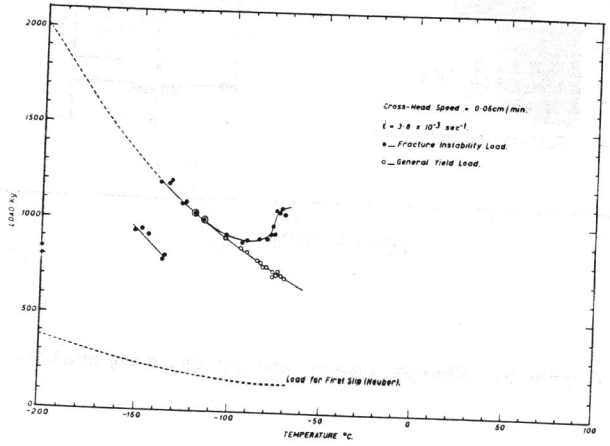

Figure 6. Fracture load-temperature diagram. Striker velocity 0.05 cm/min.

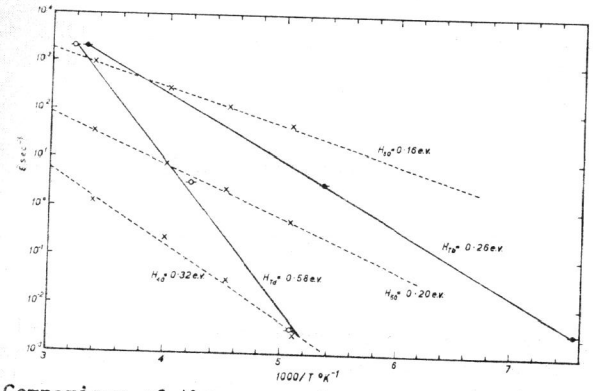

Figure 7. Comparison of the apparent activation energies for the ductility transition T_d and the bimodal transition T_d, with the activation energies for yielding at three constant stresses, 40, 50 and 60 Kg/mm^2.

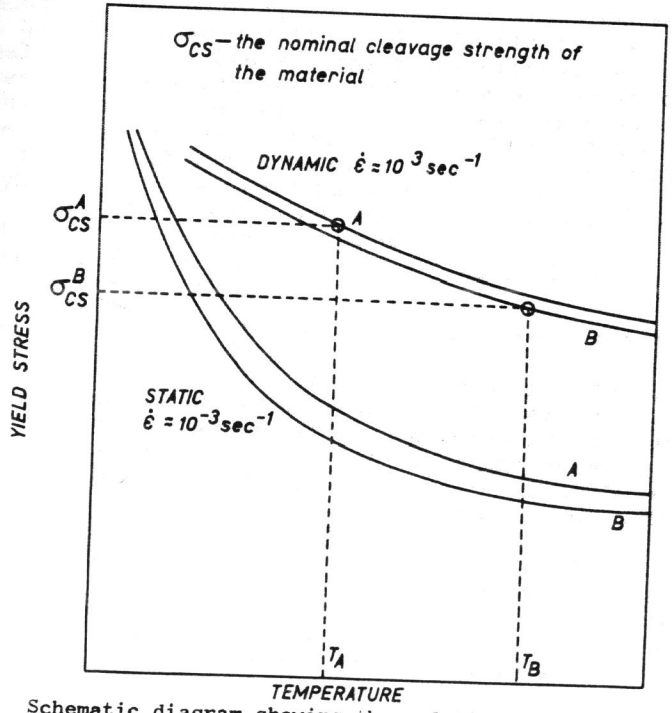

Figure 8. Schematic diagram showing the relationship between the yield stresses and the cleavage strengths of two mild steels, A and B, and their effects on the transition temperatures T_A and T_B, at two widely differing strain-rates.